J. Water Environ. Nanotechnol., 10(3): 285-296 Summer 2025

ORIGINAL RESEARCH PAPER

Phosphate Removal in Tilapia Rearing Effluent by Using CaO Catalyst Synthesized from Moaberry Pomace

Pongsathorn Tongkasee[1], Dutsadee Srithat[1], Amornrat Rangsiwiwat[2*]

[1] Department of Thai Traditional Medicine, Faculty of Natural Resources, Rajamangala University of Technology Isan Sakon Nakhon campus, Thailand
[2] Department of Fisheries, Faculty of Natural Resources, Rajamangala University of Technology Isan Sakon Nakhon campus, Thailand

Received: 2025-01-24 Accepted: 2025-04-19 Published: 2025-08-01

ABSTRACT
Water management is essential in aquaculture to ensure food security and reduce environmental impacts. This study explores the use of calcium oxide (CaO), derived from moaberry (*Antidesma thwaitesianum*) pomace, for phosphate removal in tilapia farming water. The CaO catalyst was produced by calcining moaberry pomace at 950°C for seven hours, resulting in a material with over 50% CaO content, confirmed by scanning electron microscopy (SEM) and X-ray fluorescence (XRF) analyses. When introduced into water, CaO reacts to form calcium hydroxide ($Ca(OH)_2$), which shows significant phosphate removal ability. Under white LED light (15W, 6500K), the material also acts as a photocatalyst, generating hydroxyl radicals that enhance phosphate degradation. To apply the catalyst in a practical system, it was combined with glass powder and sodium silicate to form a composite. It was then used in a continuous-flow fixed-bed photocatalytic column. During a 120-minute treatment, the system achieved a 72% reduction in phosphate concentration at 60 minutes using a 20% CaO composite. These results demonstrate the potential of LED-assisted photocatalysis as a low-energy, environmentally friendly water treatment approach. The study highlights the value of agricultural waste utilization and green photocatalytic technology in addressing eutrophication in aquaculture. Future work should focus on improving catalyst performance, optimizing operational conditions, and evaluating long-term field applications to support sustainable aquaculture practices.

Keywords: *Antidesma thwaitesianum, aquaculture waste, phosphate removal, CaO-catalyst, fixed-bed photocatalysis*

How to cite this article
Tongkasee P., Srithat D., Rangsiwiwat A. Phosphate Removal in Tilapia Rearing Effluent by Using CaO Catalyst Synthesized from Moaberry Pomace. J. Water Environ. Nanotechnol., 2025; 10(3): 285-296.
DOI: 10.22090/jwent.2025.03.004

INTRODUCTION

Tilapia farming has become an essential part of global aquaculture, contributing significantly to food production and security [1]. However, the rapid growth of this industry has led to serious challenges, particularly concerning water quality and environmental sustainability. A significant proportion of fish feed, estimated at 30%, remains uneaten and enters the aquatic environment, contributing to pollution [2]. Additionally, fish metabolic waste, containing nitrogen and phosphate, exacerbates water quality issues by promoting eutrophication—a process that depletes oxygen and damages aquatic ecosystems [3].

These problems underline the pressing need for effective, sustainable water treatment solutions to ensure the long-term viability of aquaculture. Among various innovations, photocatalysis has emerged as a promising method for addressing water contamination in aquaculture. This technique uses light-activated catalysts to break down organic pollutants and eliminate microorganisms, offering a highly efficient and environmentally

* Corresponding Author Email: *amornrat.ra@rmuti.ac.th*

This work is licensed under the Creative Commons Attribution 4.0 International License.
To view a copy of this license, visit http://creativecommons.org/licenses/by/4.0/.

friendly solution [4,5]. Photocatalytic systems are particularly effective at removing persistent pollutants, such as organic micropollutants (OMPs), which can significantly impact water quality [6]. Advances in this field, including photo-electrocatalysis, have further improved pollutant degradation by enhancing the performance and efficiency of these systems [7].

Calcium oxide (CaO) has gained attention for its role in enhancing photocatalytic processes. It can improve pollutant removal by facilitating better charge separation and increasing catalytic activity [8]. Abundant in natural and agricultural waste products, calcium-based compounds like calcium carbonate ($CaCO_3$) and CaO are cost-effective and accessible materials for large-scale applications [9]. Waste materials such as eggshells, oyster shells, and clam shells have been successfully repurposed to produce CaO, demonstrating their potential for use in water treatment [10–12]. Furthermore, activated CaO catalysts have shown excellent performance in applications ranging from methanolysis to the degradation of waterborne contaminants [13].

This study explores a novel approach to water treatment in tilapia farming, focusing on the use of CaO particles synthesized from moaberry pomace. Moaberry (*Antidesma thwaitesianum*), a fruit commonly grown in Thailand, is valued for its high phytochemical content and notable calcium levels, with calcium comprising approximately 13.30% of its composition [14–16]. During juice production, the leftover skins, pulp, and seeds from the moaberry are discarded as pomace. This pomace, which is a fruit processing byproduct, is considered agricultural waste due to its origin in the food industry and limited direct commercial value. Known for its catalytic and antimicrobial properties, CaO has been widely applied to environmental protection, material science, and medicine [17,18]. In this research, CaO was produced through calcination and thermal curing of moaberry pomace, achieving a calcium oxide content exceeding 50%, as demonstrated in the findings of Thongkasee and Rangsiwiwat [19]. By combining CaO with photocatalytic technology, this study investigates its application for phosphate removal in aquaculture water. The approach not only addresses the critical challenge of nutrient buildup in fish farming systems but also highlights the potential for transforming agricultural waste into valuable resources. This innovative method aligns with the global emphasis on sustainable practices, contributing to both environmental protection and the advancement of aquaculture. By improving water quality and promoting sustainable resource use, this research offers practical solutions for the future of aquaculture.

MATERIALS AND METHODS

Preparation of Metal Oxide from Moaberry Pomace for Catalyst Formation

Moaberry pomace powder was calcined and thermally treated at 950°C for 7 hours, as our previous study [19] described the synthesis procedure on moaberry juice processing waste for CaO production with this protocol. The SEM and XRF analysis of the conditions confirmed the maximum particle size of CaO (1.14 ± 0.41 μm) and CaO content of 54.49%, respectively, at the condition where the values are the most optimized. The energy-dispersive X-ray spectroscopy (EDX) and XRF elemental composition analysis showed calcium as the principal component, always more than 45% wt in calcination times. This confirms that the material is suitable for further catalytic applications, in concordance with the CaO content in other high-calcium-rich ashes reported after calcination, that is, orange peel ash [20] and incense stick ash [21].

Finely ground recycled glass powder was mixed with moaberry pomace powder for catalyst preparation. Sodium silicate (Na_2SiO_3) was added as a binder [22], and the mixture was molded and cured at 60°C for 24 hours. The catalyst was prepared in ratios of 10, 15, and 20 w/w% moaberry pomace powder to glass powder to evaluate the optimal concentration for phosphate removal [23,24].

This experiment utilized finely ground glass powder from clean, dried recycled glass bottles, which were proportionally mixed with moaberry pomace powder. The inclusion of optimized components of the glass powder helps prevent deformation and enhances anti-corrosion properties [25]. Based on previous studies, the effective concentration of the catalyst ranges from 0.1 to 20 w/w% [26,27]. In this current study, the chosen range is 10-20 w/w%.

Removal of Phosphate in Water from Tilapia Rearing Effluent.

A study was conducted to evaluate phosphate ion removal in water from tilapia rearing in earthen ponds, following the method of Vijuksungsith et al. [28]. As phosphate speciation and reactivity can

CC BY

Table 1. presents the key physicochemical properties of the phosphate ion (PO_4^{3-})

Property	Value	Unit / Remark
Chemical formula	PO_4^{3-}	
Molecular weight	94.97	g/mol
Ionic radius (P^{5+})	0.17	nm
Formal charge	−3	
Solubility (as $Na_3PO_4{\cdot}12H_2O$)	28.3	g/100 mL at 25°C (in water)
Solubility product (Ksp of $Ca_3(PO_4)_2$)	~2.07×10^{-33}	Very low; indicates limited solubility in water
Acid dissociation constants (pKa)	$pKa_1 = 2.15$, $pKa_2 = 7.20$, $pKa_3 = 12.35$	Refers to stepwise deprotonation of H_3PO_4
Common oxidation state of phosphorus	+5	
Electronegativity (Pauling scale)	2.19	
Molecular geometry	Tetrahedral	P central, four O at vertices

Note: These physicochemical properties influence the mobility, reactivity, and interaction of phosphate ions with calcium-based materials under typical water treatment conditions. Data for molecular weight, ionic radius, electronegativity, and solubility were obtained from standard chemical data compilations [29], while pK_a values, solubility product (Ksp), and speciation behavior were referenced from aquatic chemistry literature [30].

influence removal efficiency in aquaculture systems, Table 1 outlines the physicochemical properties of PO_4^{3-} that are pertinent to its behavior in tilapia pond water.

The study compared the phosphate ion removal in natural water samples from farm ponds with water samples to which a phosphate solution was added to reach a concentration of 100 mg/L. The water used in this experiment was obtained from tilapia farms in Sakon Nakhon, Thailand (17°16′48.72″N, 103°55′42.73″E), where tilapia was reared in earthen ponds with a stocking density of 10 fish/m² for 6 months. Water samples were collected before harvesting, and no changes were made to the water quality before analysis. Upon arrival at the water quality analysis facility, the farm water samples exhibited the following parameters: pH 4.80 ± 0.61, conductivity (EC) 0.45 ± 0.17 µS/cm, total dissolved solids (TDS) 237.08 ± 32.40 mg/L, and dissolved oxygen (DO) 3.92 ± 0.46 mg/L by YSI Model: 556 MPS. Total Phosphate (TPP) 23.14 ± 0.59 mg/L measured according to [31].

Application of CaO Photocatalyst to Water Treatment

CaO was applied in a continuous flow fixed-bed column system, reacting with water to form $Ca(OH)_2$ as shown (1)

$$CaO + H_2O \rightarrow Ca(OH)_2 \quad (1)$$

$Ca(OH)_2$ releases calcium ions, which bind with phosphate ions to form insoluble tricalcium phosphate (2)

$$3Ca_{2^+} + 2PO4_{3^-} \rightarrow Ca_3(PO4)_2 \downarrow \quad (2)$$

These precipitates effectively reduce the concentration of phosphate in the water, aiding in the prevention of eutrophication and contributing to improved water quality.

The system operated at a flow rate of 15 L/min and a column height of 10 cm, maintaining natural pH and room temperature conditions as described in [28]. The catalyst was exposed to 6500K LED illumination, which facilitated photocatalytic reactions producing hydroxyl radicals and superoxide ions (Equations 3–6), thereby enhancing pollutant degradation.

$$\text{Photocatalyst} + hv(LED\,light) \rightarrow e^- + h^+ \quad (3)$$

$$h^+ + H_2O \rightarrow \cdot OH + H^+ \quad (4)$$

or

$$h^+ + OH^- \rightarrow \cdot OH \quad (5)$$

$$e^- + O_2 \rightarrow O_{2^-} \quad (6)$$

Experimental Setup and Analysis

Water samples were collected at 10, 30, 60, and 120 minutes to analyze phosphate levels (Fig. 1).

The experiment included three treatments and a control:

Control: The water flowed through the column without a catalyst

Treatment 1: The water flowed through the catalyst column containing 10% CaO

Treatment 2: The water flowed through the catalyst column containing 15% CaO

(cc) BY

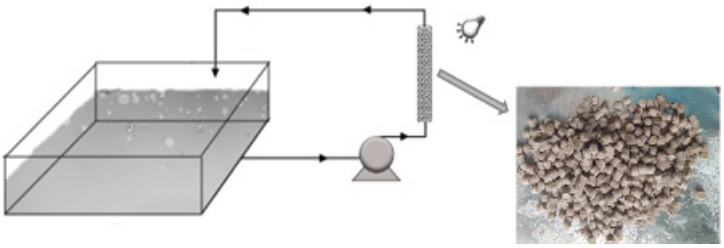

Fig. 1. Experimental setup for evaluating photocatalyst efficiency in water treatment

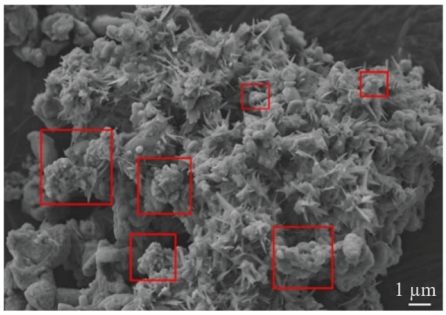

Fig. 2. SEM of moaberry pomace, calcined at 950°C for 7 hours

Treatment 3: The water flowed through the catalyst column containing 20% CaO

The LED-activated test used a Neox LED 15W 1500LM Day Light 6500K as the light source at room temperature. LEDs are energy-efficient and cost-effective, and emit 400-500 nm wavelengths visible as white light, effectively enhancing photocatalyst activation for pollutant degradation. They offer stable light with minimal heat, create ideal reaction conditions, and are environmentally friendly, containing no hazardous materials [32,33].

Samples were collected at 10, 30, 60, and 120 minutes under the following conditions:

Control: The water flowed through the column without a catalyst and an LED

Treatment 1: The water flowed through the catalyst column without an LED

Treatment 2: The water flowed through the catalyst column containing with LED

Statistical Analysis

Phosphate removal (%) was calculated based on the initial and final concentrations of total phosphate according to Eq.7 [34].

$$\%Removal = \frac{\left((Ci - Cf) \times 100\right)}{Ci} \quad (7)$$

Where Ci and Cf are the initial and final concentrations.

The experimental results were expressed as mean value ± standard deviation (mean ± SD). Statistical analysis was conducted using the package 'stats' in R program version 4.4.1 for Windows [35]. Significant differences between treatments were determined using a two-way analysis of variance (Two-way ANOVA) test with a confidence level of 95% (p-value < 0.05).

RESULTS AND DISCUSSION

Characterization of CaO Catalyst

SEM measurements indicated a particle size of 1.14 ± 0.41 µm [19], contributing to an increased surface area essential for efficient phosphate adsorption (Fig. 2)

The CaO-based catalyst synthesized using 20% moaberry pomace powder exhibited distinct surface characteristics. SEM imaging revealed that the CaO particles primarily assumed a rounded morphology, which was heterogeneously distributed within a matrix of finely pulverized glass fragments. These glass inclusions were polygonal to rod-shaped, contributing to a heterogeneous microstructure (Fig. 3). This specific structural arrangement plays a crucial role in enhancing the material's adsorption efficiency. The increased surface area, resulting from the rounded and rod-shaped, provides more active sites for phosphate

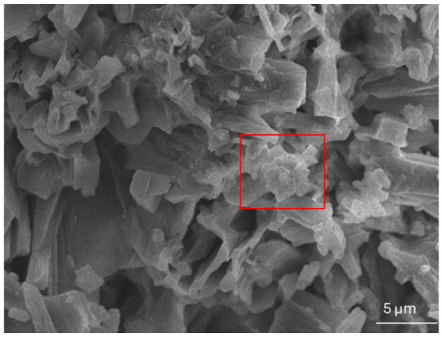

Fig. 3. SEM of the CaO catalyst mixed with glass fragments

Table 2. Comparison of surface area, pore characteristics, and isotherm properties of CaO catalysts prepared with different concentrations (10%, 15%, and 20%).

Parameter	10% CaO	15% CaO	20% CaO
BET Surface Area (m^2/g)	0	0.853*	0
BJH Surface Area (Des) (m^2/g)	1.072	-	1.433
DH Surface Area (Des) (m^2/g)	1.231	-	1.592
DFT Surface Area (m^2/g)	0.26	-	0.884
BJH Pore Volume (cc/g)	0.001583	-	0.002748
BJH Pore Radius (Å)	22.7	approx. 25**	29.97
Isotherm Pattern	Irregular	Moderate	Type IV + H3 loop

binding, significantly improving the catalyst's performance during water treatment processes. Additionally, the integration of glass fragments within the CaO matrix contributes to the material's mechanical strength. This reinforcement ensures that the catalyst remains stable and effective over prolonged use in continuous-flow water treatment systems.

Textural and Surface Properties of CaO Catalysts

Textural properties of CaO catalysts synthesized with 10%, 15%, and 20% loadings were characterized to evaluate their suitability for phosphate removal (Table 2). The 15% CaO catalyst exhibited the highest BET surface area (0.853 m^2/g), indicating moderate porosity. However, BET surface area was undetectable in the 10% and 20% CaO formulations, likely due to pore blockage or particle agglomeration during calcination. Despite this, pore radius analysis revealed important differences among the samples.

Notably, the 20% CaO catalyst demonstrated a BJH pore radius of 29.97 Å, which falls within the mesoporous range according to the IUPAC classification (2–50 nm). Its nitrogen adsorption–desorption isotherm displayed a Type IV pattern with an H3 hysteresis loop—both characteristics typical of mesoporous materials with slit-like pores formed by aggregated plate-like particles [36,37,38]. In contrast, the 10% and 15% CaO catalysts showed less-defined pore structures, with the 10% sample exhibiting irregular isothermal behavior.

Although the 15% CaO had a higher surface area, the 20% CaO catalyst achieved the highest phosphate removal efficiency under both adsorption and photocatalytic conditions. This suggests that mesoporous structure and pore accessibility play a more significant role in catalytic performance than surface area alone.

Efficiency of Catalyst-Assisted Phosphate Adsorption in Tilapia Rearing Effluent

The results of the two-way ANOVA (Table 3) demonstrate that both catalyst concentration and exposure time significantly influenced phosphate removal in tilapia farming water. Importantly, the lack of a significant interaction between these two variables indicates that their effects are independent. In contrast, the presence of a statistically significant interaction (p-value < 0.001) suggests that the effect of catalyst concentration on phosphate removal efficiency depends on the duration of exposure. This finding implies that catalyst concentration and exposure time each contribute separately to phosphate removal efficiency, allowing for individual optimization of

Table 3. Two-way ANOVA summary on the efficiency of catalyst-assisted phosphate absorption in treated water from tilapia rearing effluent.

	Df	Sum Sq	Mean Sq	F value	Pr(>F)
Concentration	3	3058.20	1019.40	748.90	0.000 ***
Time	3	1856.93	618.97	454.73	0.000 ***
Conc=Time	9	817.76	90.86	66.75	0.000 ***
Residuals	32	43.56	1.361		
R^2	0.99				
Adjusted R^2	0.98				

Significance codes: 0 '***' 0.001 '**' 0.01 '*' 0.05 '.' 0.1 ' ' 1

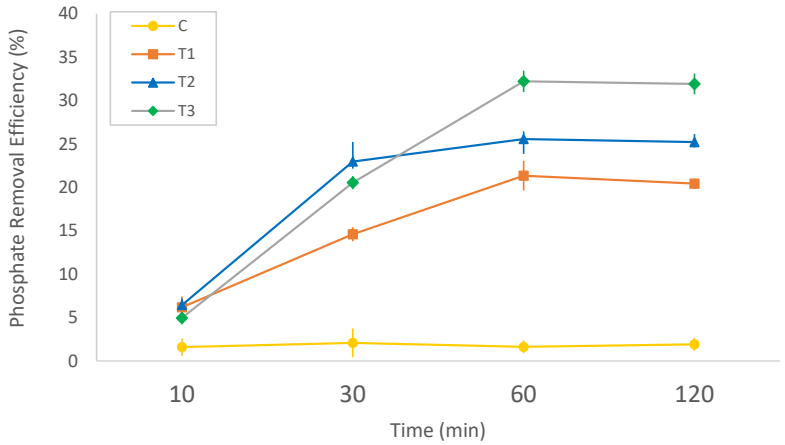

Fig. 4. The percentage of phosphate removal in the water in tilapia rearing effluent when flowing through the column with a catalyst containing continuous (C = Control: without a catalyst, T1: the catalyst column containing 10% CaO, T2: the catalyst column containing 15% CaO, T3: the catalyst column containing 20% CaO)

these parameters without compromising overall performance. Therefore, the combined effect must be considered when optimizing treatment conditions to achieve maximum removal. Catalyst concentration had a statistically significant effect on phosphate removal rates (p-value < 0.000), confirming that higher concentrations of active material substantially enhance the adsorption process. Similarly, exposure time also showed a significant effect (p-value < 0.000), underscoring the critical role of treatment duration in achieving effective phosphate removal. The interaction between catalyst concentration and exposure time was highly significant (p-value < 0.000), indicating that the combined effect of these variables must be evaluated in tandem. The very low residual mean square of 0.8 reflects the high precision of the model in explaining the variability in phosphate removal. The coefficient of determination (R^2) of 0.99 indicates that 99% of the variation in phosphate removal efficiency can be explained by the experimental factors. These findings align with previous studies, which indicate that increasing the concentration of active materials improves adsorption by providing a greater number of binding sites for phosphate molecules [39]

The phosphate adsorption efficiency of the synthesized catalyst was particularly evident when water passed through a column containing 20% CaO. Under these conditions, a 32% reduction in phosphate levels was achieved within just 60 minutes (Fig. 4). This performance underscores the potential of the 20% CaO catalyst to provide a practical and efficient solution for managing nutrient pollution in aquaculture systems. Compared to the control and lower catalyst levels (T1 and T2), the T3 treatment (20% CaO) demonstrated the highest removal efficiency across all time points.

The rapid adsorption within the first 60 minutes further highlights the material's suitability for short-contact-time treatment applications.

Phosphate Removal by LED-Activated CaO Photocatalyst in Tilapia Rearing Effluent

The observed phosphate removal efficiency was statistically supported by the two-way ANOVA results (Table 4), which showed significant effects

(cc) BY

Table 4. Two-way ANOVA summary of phosphate removal efficiency using LED-activated CaO photocatalyst in Tilapia rearing effluent.

	Df	Sum Sq	Mean Sq	F value	Pr(>F)
Concentration	2	10891.08	5445.54	289.73	0.000 ***
Time	3	5644.33	1881.44	100.10	0.000 ***
Conc=Time	6	3887.62	647.93	34.47	0.000 ***
Residuals	24	451.07	17.79		
R^2	0.97				
Adjusted R^2	0.96				

Significance codes: 0 '***' 0.001 '**' 0.01 '*' 0.05 '.' 0.1 ' ' 1

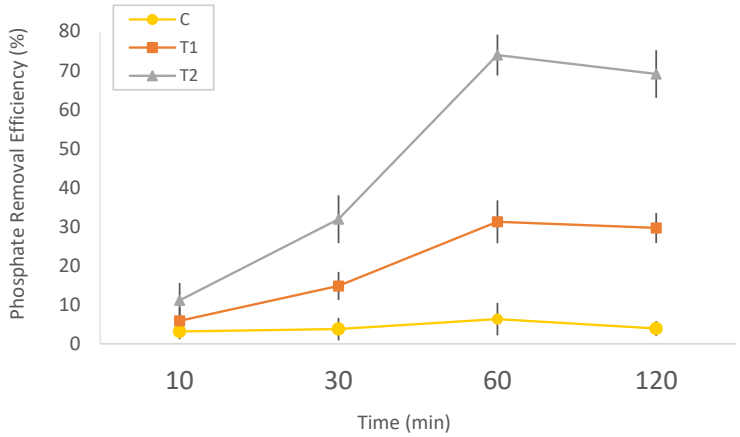

Fig. 5. The percentage of phosphate removal (%) where water was passed through a column containing different catalytic treatments. C represents the control group without any catalyst or LED exposure; T1 represents the use of a 20% CaO catalyst column without LED light; and T2 indicates the application of a 20% CaO catalyst column under LED illumination.

of catalyst concentration, exposure time, and their interaction ($p < 0.001$). The coefficient of determination ($R^2 = 0.97$) further confirms the robustness of the model in explaining the variation in removal performance.

The use of an LED-activated CaO catalyst in a continuous-flow fixed-bed column resulted in a 72% reduction in phosphate levels within 60 minutes (Fig. 5). This significant reduction aligns with the critical goals of water treatment in aquaculture, where controlling phosphate levels is essential to prevent eutrophication and maintain sustainable water quality. The results highlight the potential of this method as a practical and scalable solution for improving the environmental sustainability of aquaculture systems. The effectiveness of white LED light in facilitating photocatalytic reactions was evident in this study. White LEDs offer several advantages for water treatment applications, including energy efficiency, low heat generation, and stable illumination. These properties enhance photocatalytic activity, making white LEDs a reliable and sustainable choice for promoting pollutant degradation. Despite common concerns about the performance of low-intensity LEDs, the present study achieved over 70% phosphate removal under white LED illumination. Alternative configurations like phosphorus-doped carbon nitride nanosheets have demonstrated stable and high pollutant removal efficiencies under white LED illumination. This reinforces the suitability of white LEDs for sustainable wastewater treatment applications [40].

This study highlights not only the effectiveness of LED-activated CaO in removing phosphate but also its potential as a low-energy solution for treating aquaculture wastewater. Experimental comparisons indicated that adsorption contributed approximately 32% to overall phosphate removal, with photocatalytic degradation responsible for an additional 40%. These findings align with previous research showing that calcium-rich metal oxides operate via both adsorption and photocatalytic pathways under visible light exposure [10,30]. LED-assisted phosphate removal offers a sustainable alternative that reduces chemical input while supporting environmentally friendly practices in tilapia aquaculture.

The comparative analysis of various CaO-based materials (Table 5) demonstrates diverse efficiencies

(cc) BY

Table 5. Comparison of phosphate removal efficiency by various CaO-based

Catalyst type	Efficiency (%) or Capacity (mg/g)	Conditions	Mechanism type	Reference
$CaCO_3$-SBA-15 composite	92.0 mg/g	Mesoporous nanocomposite, Ca: Si = 0.55	Adsorbent	[41]
Ag/CaO-AC nanocomposite	77.4 mg/g	45 min, 0.02 g dose, 40 mg/L phosphate	Adsorbent	[42]
Cement/slag/coal ash hydrate	>90%	Hydrated cementitious material	Adsorbent (CaO-releasing)	[43]
CaO_2/UV system	97% (hypophosphite)	UV-assisted CaO_2, 6 h	Photocatalyst	[44]
Activated carbon–based	85%	Batch: aquaculture water	Photocatalyst	[28]
Shell-derived	90%	Adsorption in lab-scale AOP	Photocatalyst	[11]
Moaberry pomace CaO	72%	LED 6500K, fixed-bed, 20% wt	Dual: Adsorption (32%) + Photocatalysis (40%)	This study

and mechanisms for phosphate removal. Among the adsorbent systems, the $CaCO_3$-SBA-15 composite exhibited the highest phosphate adsorption capacity at 92.0 mg/g [41], followed by the Ag/CaO-AC nanocomposite with 77.4 mg/g under a 45-minute contact time and a 0.02 g dose at 40 mg/L phosphate concentration [42]. Additionally, the cement/slag/coal ash hydrate-based material achieved over 90% phosphate removal efficiency through a dual mechanism involving both adsorption and CaO release [43]. Photocatalytic approaches, including the CaO_2/UV system, achieved phosphate removal efficiency as high as 97% [44], while activated carbon–based CaO catalysts also demonstrated strong performance in aquaculture water treatment [28]. Shell-derived CaO photocatalysts further support the versatility of CaO materials in advanced oxidation processes [11]. Notably, the CaO synthesized from moaberry pomace in this study combined both adsorption and photocatalysis, achieving a total removal efficiency of 72%. This dual-function mechanism has the benefit of treating both ionic phosphate and presumed organic-bound phosphorus compounds. More importantly, preproduction of CaO from agricultural waste further demonstrates that this could promote the sustainability and environmental benefits of these catalysts for aquaculture water remediation.

Comparative Approaches in Water Treatment

In this study, a dual-function phosphate removal approach integrating adsorption and photocatalysis was developed. At 20% CaO-glass input, 32% removal was observed under dark conditions, increasing to 72% under LED illumination. These findings indicate that photocatalytic reactions, activated by light, significantly enhance removal efficiency beyond the adsorption baseline. This dual-mode mechanism aligns with previous reports on the synergistic effects of adsorption and advanced oxidation processes (AOPs) for phosphate elimination [45]. Such hybrid systems underscore the importance of combining multiple removal pathways to optimize water treatment. Effective pollutant removal strategies are critical for maintaining water quality in aquaculture systems. For instance, iron oxide/activated carbon nanoparticles have been shown to efficiently remove heavy metals from water [46]. Similarly, silica nanoparticles derived from rice husks have demonstrated notable lead adsorption performance in tilapia farming environments [47].

Biochar derived from crab shells has demonstrated remarkable effectiveness in eliminating malachite green residues from water, further highlighting the utility of natural by-products in environmental applications [48]. Activated carbon produced from Bambusa vulgaris var. striata has also been proven to effectively remove mercury ions (Hg^{2+}), illustrating the versatility of plant-derived materials for water treatment [49]. Additionally, Biological Aerated Filters integrated with Marchantia polymorpha have been successfully applied to treat ammonia nitrogen, reinforcing the importance of sustainable and integrated waste management practices in aquatic environments [50].

These comparative examples highlight the growing potential of using agricultural by-

(cc) BY

products as cost-effective and sustainable solutions for pollutant removal. In this context, the use of calcium oxide (CaO) synthesized from moaberry pomace represents an innovative and practical approach. By leveraging the adsorption properties of CaO, this method provides a valuable pathway for improving water quality in aquaculture while promoting the upcycling of agricultural waste. Such approaches contribute to the development of sustainable, efficient, and environmentally friendly solutions for water treatment.

Limitations and Future Research

The observed 72% phosphate removal rate demonstrates promising potential but also highlights opportunities for further improvement. Future studies should focus on enhancing the catalyst's surface area using advanced material engineering techniques, such as templating or incorporating porous support materials. These approaches can increase active sites for adsorption and improve overall efficiency [51]. Additionally, optimizing water flow through computational fluid dynamics (CFD) modeling could ensure uniform catalyst contact and minimize channeling effects, thereby enhancing performance [52]. Testing catalyst performance under diverse environmental conditions would help identify concentration thresholds for maximum efficiency, providing a clearer understanding of its optimal application [53]. Furthermore, adjustments to LED light intensity [54] and investigations into the effects of environmental factors, such as pH and temperature, could yield additional performance gains [55]. The precipitation of calcium hydroxide as calcium phosphate is a critical mechanism for reducing phosphate levels and mitigating eutrophication risks. Supporting evidence includes studies demonstrating high phosphorus adsorption capacity in thermally treated water treatment sludge (WTS) [56]. Similarly, sepiolite/ZrO_2 composites forming inner-sphere complexes and zirconium-modified porous nanowood retaining over 80% efficiency across multiple adsorption cycles highlight effective phosphate removal strategies [57]. Optimized pH conditions have also been shown to improve phosphorus removal rates to as high as 98% using steel-making slag, offering valuable insights into enhancing adsorption processes [58].

Although the present study was performed to evaluate the initial activity of moaberry pomace-derived CaO for phosphate removal, studies on its reusability and photocatalyst structuring in response to adsorption–photocatalysis should be addressed for future research. This is important for the potential long-term application of the catalyst in aquaculture water treatment systems by assessing the regeneration potential and stability of the catalyst. Finally, data describing the cost–benefit analyses of employing moaberry pomace-derived CaO in aquaculture in real-world scales should be generated in future studies. These assessments will inform on the potential of such a large deployment and any emerging trade-offs between environmental and financial endpoints.

CONCLUSIONS

This study demonstrates the potential of CaO synthesized from moaberry juice by-product waste as an effective and sustainable material for water treatment in aquaculture. By converting agricultural by-products into functional resources, this approach exemplifies the circular economy principles, addressing waste management challenges while mitigating eutrophication risks in aquatic environments. The results underline the feasibility of using moaberry pomace-derived CaO for improving water quality and supporting sustainable aquaculture practices.

Future research should prioritize optimizing the physical and chemical characteristics of the catalyst to enhance its efficiency and durability. Refining operational conditions, such as flow rates, light intensity, and environmental parameters, will further improve its applicability and performance. Additionally, efforts should focus on scaling this technology to accommodate real-world implementation in larger aquaculture systems. Advancing these areas will contribute to the development of practical, cost-effective, and eco-friendly solutions for sustainable water treatment in aquaculture and beyond.

ACKNOWLEDGEMENTS

This project could not have been completed without the funding from the National Research Council of Thailand, Project ID: SKC2562REV058, and the support from the Faculty of Natural Resources, Rajamangala University of Technology Isan, Sakon Nakhon Campus. Their provision of facilities and equipment was instrumental in conducting this research. The writing of this manuscript benefited from review by the

(cc) BY

AQUADAPT-Nature project, supported by the Government of Canada's International Climate Finance Initiative and the International Development Research Centre, Ottawa, Canada.

CONFLICT OF INTEREST

The authors declare no conflict of interest.

REFERENCES

1. Sampathkumar K, Yu H, Loo SCJ. Valorisation of industrial food waste into sustainable aquaculture feeds. Future Foods. 2023;7:100240. https://doi.org/10.1016/j.fufo.2023.100240
2. Debnath SC, McMurtrie J, Temperton B, Debouttеville JD, Mohan CV, Tyler CR. Tilapia aquaculture, emerging diseases, and the roles of the skin microbiomes in health and disease. Aquac Int. 2023;31:2945–76. https://doi.org/10.1007/s10499-023-01117-4
3. Bueno GW, Bernal FEM, Roubach R, Skipper-Horton JO, Sampaio FG, Fialho NS, et al. Mathematical modeling of waste outputs in the aquatic environment from commercial cage farms under neotropical climate conditions. Aquac Environ Interact. 2023;15:133–44. https://doi.org/10.3354/aei00457
4. Astuti LP, Sugianti Y, Warsa A, Sentosa AA. Water quality and eutrophication in Jatiluhur Reservoir, West Java, Indonesia. Pol J Environ Stud. 2022;31(2):1493–503. https://doi.org/10.15244/pjoes/142475
5. Yang Y, Li X, Zhou C, Xiong W, Zeng G, Huang D, et al. Recent advances in application of graphitic carbon nitride-based catalysts for degrading organic contaminants in water through advanced oxidation processes beyond photocatalysis: A critical review. Water Res. 2020;184:116200. https://doi.org/10.1016/j.watres.2020.116200
6. Kocijan M, Ćurković L, Gonçalves G, Podlogar M. The potential of rGO@TiO_2 photocatalyst for the degradation of organic pollutants in water. Sustainability. 2022;14:12703. https://doi.org/10.3390/su141912703
7. Ben-Asher R, Gendel Y, Lahav O. Electrochemical applications in RAS: A review. Rev Aquac. 2023;16(1):86–105. https://doi.org/10.1111/raq.12822
8. Ibhadon AO, Fitzpatrick P. Heterogeneous photocatalysis: Recent advances and applications. Catalysts. 2013;3(1):189–218. https://doi.org/10.3390/catal3010189
9. Su H, Guo X, Zhang X, Zhang Q, Huang D, Lin L, et al. Ultrafine biosorbent from waste oyster shell: A comparative study of Congo red and methylene blue adsorption. Bioresour Technol Rep. 2022;19:101124. https://doi.org/10.1016/j.biteb.2022.101124
10. Narayan RB, Goutham R, Srikanth B, Gopinath KP. A novel nano-sized calcium hydroxide catalyst prepared from clam shells for the photodegradation of methyl red dye. J Environ Chem Eng. 2018;6(3):3640–7. https://doi.org/10.1016/j.jece.2016.12.004
11. Risso R, Ferraz P, Meireles S, Fonseca I, Vital J. Highly active CaO catalysts from waste shells of egg, oyster and clam for biodiesel production. Appl Catal A Gen. 2018;567:56–64. https://doi.org/10.1016/j.apcata.2018.09.003
12. Kurian M. Cerium oxide-based materials for water treatment – A review. J Environ Chem Eng. 2020;8(5):104439. https://doi.org/10.1016/j.jece.2020.104439
13. Guo S, Wang H, Wei Y, Fida H, You L, Zhou K. Scalable synthesis of Ca-doped α-Fe_2O_3 with abundant oxygen vacancies for enhanced degradation of organic pollutants through peroxymonosulfate activation. Appl Catal B. 2020;262:118250. https://doi.org/10.1016/j.apcatb.2019.118250
14. Jorjong S, Butkhup L, Samappito S. Phytochemicals and antioxidant capacities of Mao-Luang (Antidesma bunius L.) cultivars from Northeastern Thailand. Food Chem. 2015;181:248–55. https://doi.org/10.1016/j.foodchem.2015.02.093
15. Butkhup L, Samappito S. Analysis of anthocyanin, flavonoids, and phenolic acids in tropical bignay berries. Int J Fruit Sci. 2008;8:15–44. https://doi.org/10.1080/15538360802365913
16. Puangpronpitag D, Yongvanit P, Boonsiri P, Suttajit M, Areejitranusorn P, Na HK, et al. Molecular mechanism underlying anti-apoptotic and anti-inflammatory effects of Mamao (Antidesma thwaitesianum Müll. Arg.) polyphenolics in human breast epithelial cells. Food Chem. 2011;127(4):1450–8. https://doi.org/10.1016/j.foodchem.2011.01.099
17. Jadhav V, Bhagare A, Wahab S, Lokhande D, Vaidya C, Dhayagude A, et al. Green synthesized calcium oxide nanoparticles (CaO NPs) using leaves aqueous extract of Moringa oleifera and evaluation of their antibacterial activities. J Nanomater. 2022;9047507. https://doi.org/10.1155/2022/9047507
18. Lesbani A, Sitompul SOC, Mohadi R, Hidayati N. Characterization and utilization of calcium oxide (CaO) thermally decomposed from fish bones as a catalyst in the production of biodiesel from waste cooking oil. Makara J Technol. 2016;20(3):121–6. https://doi.org/10.7454/mst.v20i3.3066
19. Thongkasee P, Rangsiwiwat A. Synthesis and characterization of CaO based on Moa residue. In: Proc 11th Rajamangala Surin Natl Conf; 2020; Surin, Thailand. p. 89–97. [in Thai]
20. Pérez S, Giraldo S, Forgionny A, Flórez E, Acelas N. Eco-friendly reuse of agricultural wastes to produce biocomposites with high potential in water treatment and fertilizers. Biomass Convers Biorefin. 2024;14:8537–47. https://doi.org/10.1007/s13399-022-02948-6
21. Sun H, Sun K, Wang F, Liu Y, Ding L, Xu W, et al. Catalytic self-activation of Ca-doped coconut shell for in-situ synthesis of hierarchical porous carbon supported CaO transesterification catalyst. Fuel. 2021;285:119192. https://doi.org/10.1016/j.fuel.2020.119192
22. LaFa V. Application of no-bake sodium silicate binder systems. Int J Metalc. 2012;6(3):19–26. https://doi.org/10.1007/BF03355530
23. Gu Y, Xie D, Ma Y, Qin W, Zhang H, Wang G, et al. Size modulation of zirconium-based metal-organic frameworks for highly efficient phosphate remediation. ACS Appl Mater Interfaces. 2017;9(37):32151–60. https://doi.org/10.1021/acsami.7b10024
24. Winkler P, Raab M, Zeininger J, Rois LM. Imaging interface and particle size effects by in situ correlative microscopy of a catalytic reaction. ACS Catal. 2023;13:7650–60. https://doi.org/10.1021/acscatal.3c00060
25. Jabed A, Khan MM, Camiller J. Property optimization of Zr-Ti-X (X=Ag, Al) metallic glass via combinatorial development aimed at prospective biomedical application. Surf Coat Technol. 2019;372:278–87. https://doi.org/10.1155/2022/9047507
26. Kobayashi Y, Kanasaki R, Nozaki T, Shoji R, Sato K. Im-

CC BY

proving effect of MnO_2 addition on TiO_2-photocatalytic removal of lead ion from water. J Water Environ Technol. 2017;15(2):35–42. https://doi.org/10.2965/jwet.16-021
27. Yang C, Zhang C, Chen ZJ, Li Y, Yan WY, Yu HB, et al. Three-dimensional hierarchical porous structures of metallic glass/copper composite catalysts by 3D printing for efficient wastewater treatments. ACS Appl Mater Interfaces. 2021;13(6):7227–37. https://doi.org/10.1021/acsami.0c20832
28. Vijuksungsith P, Satapanajar T, Chokejaroenrat C, Jarusutthirak C, Sakulthaew C, Kambhu A, et al. Removal and reuse of phosphorus from aquaculture water using activated carbon-based CaO. Environ Technol Innov. 2023;29:102990. https://doi.org/10.1016/j.eti.2022.102990
29. Lide DR, editor. CRC Handbook of Chemistry and Physics. 86th ed. Boca Raton: CRC Press; 2005.
30. Stumm W, Morgan JJ. Aquatic Chemistry: Chemical Equilibria and Rates in Natural Waters. 3rd ed. New York: Wiley-Interscience; 1996.
31. APHA-AWWA-WEF. Standard Methods for the Examination of Water and Wastewater. 22nd ed. Washington DC: American Public Health Association/American Water Works Association/Water Environment Federation; 2012.
32. Vaiano V. Visible light active photocatalysts for environmental remediation and organic synthesis. Photochem. 2022;2:225–36. https://doi.org/10.3390/photochem2010017
33. Qamar MT, Iqbal S, Aslam M, Alhujaily A, Bilal A, Rizwan K, et al. Transition metal doped CeO_2 for photocatalytic removal of 2-chlorophenol in the exposure of indoor white light and antifungal activity. Front Chem. 2023;11:1126171. https://doi.org/10.3389/fchem.2023.1126171
34. Abdelbassit MS, Alhooshani KR, Saleh TA. Silica nanoparticles loaded on activated carbon for simultaneous removal of dichloromethane, trichloromethane, and carbon tetrachloride. Adv Powder Technol. 2016;27(4):1719–29. https://doi.org/10.1016/j.apt.2016.06.003
35. R Core Team. R: A language and environment for statistical computing. Vienna: R Foundation for Statistical Computing; 2024. Available from: https://cran.r-project.org/web/packages/twowaytests/index.html [Accessed February 2024].
36. Zhang Y, Tang Q, Sun Y, Yao C, Yang Z, Yang W. Improved utilization of active sites for phosphorus adsorption in FeOOH/anion exchanger nanocomposites via a glycol-solvothermal synthesis strategy. J Environ Sci (China). 2022;111:313–23. https://doi.org/10.1016/j.jes.2021.04.018
37. Sing KSW, Everett DH, Haul RAW, Moscou L, Pierotti RA, Rouquérol J, et al. Reporting physisorption data for gas/solid systems with special reference to the determination of surface area and porosity. Pure Appl Chem. 1985;57(4):603–19. https://doi.org/10.1351/pac198557040603
38. Rouquerol F, Rouquerol J, Sing K, Llewellyn P, Maurin G. Adsorption by Powders and Porous Solids: Principles, Methodology and Applications. 2nd ed. London: Academic Press; 2014.
39. IUPAC. Manual of Symbols and Terminology for Physicochemical Quantities and Units, Appendix II: Definitions, Terminology and Symbols in Colloid and Surface Chemistry. Pure Appl Chem. 2006;79(10):1901–5. https://doi.org/10.1351/pac200779101901
40. Chi X, Tan S, Song J, Liu F, Tian Y, Yuan H, et al. Phosphorus-doped carbon nitride nanosheets as efficient white-LED-light-driven photocatalyst for hydrogen evolution and tetracycline degradation. Catal Lett. 2021;151(12):3592–602. https://doi.org/10.1007/s10562-021-03595-8
41. Nyakairu GW, Oloro J, Ntale M, Eilu P, Mukiibi R. Removal of phosphate from wastewater using silver nanoparticles–calcium oxide–activated carbon (Ag/CaO-AC) nanocomposite: Kinetics, isotherms, and thermodynamic studies. Adv Environ Eng Res. 2023;4(2):033. https://doi.org/10.21926/aeer.2302033
42. Tang YY, Wang H, Sun W, Li D, Wu ZF, Feng Y, Xu N. Synthesis of calcium carbonate-loaded mesoporous SBA-15 nanocomposites for removal of phosphate from solution. Environ Sci Pollut Res Int. 2023. https://doi.org/10.1007/s11356-023-28226-0
43. Chen L, Gao F, Zhang T. Hydrated cementitious composites for high-efficiency phosphorus removal: A circular waste solution. J Environ Manage. 2024;348:119365. https://doi.org/10.1016/j.jenvman.2023.119365
44. Zhang J, Liu Q, Chen H, Zhao X. Phosphorus recovery via UV-activated calcium peroxide: Mechanistic insights and removal kinetics. Chem Eng J. 2023;457:141233. https://doi.org/10.1016/j.cej.2023.146633
45. Yang C, Zhang C, Chen ZJ, Li Y, Yan WY, Yu HB, Liu L. Mechanism of phosphate removal by adsorption and advanced oxidation processes (AOPs). Water Res. 2007;41(15):3497–506. https://doi.org/10.1016/j.watres.2007.03.039
46. Jain M, Yadav M, Kohout T, Lahtinen M, Garg VK, Sillanpää M. Development of iron oxide/activated carbon nanoparticle composite for the removal of Cr(VI), Cu(II) and Cd(II) ions from aqueous solution. Water Resour Ind. 2018;20:54–74. https://doi.org/10.1016/j.wri.2018.10.001
47. El-Gazzar N, Almanaa T, Reda R, Gaafary M, Rashwan A, Mahsoub F. Assessment of the use of silica nanoparticles (SiO_2NPs) biosynthesized from rice husks by Trichoderma harzianum MF780864 as a water lead adsorbent for immune status of Oreochromis niloticus. Saudi J Biol Sci. 2021;28:5119–30. https://doi.org/10.1016/j.sjbs.2021.05.027
48. Wu J, Yang J, Feng P, Wen L, Huang G, Xu C, Lin B. Highly efficient and ultra-rapid adsorption of malachite green by recyclable crab shell biochar. J Ind Eng Chem. 2022;113:206–14. https://doi.org/10.1016/j.jiec.2022.05.047
49. Alfatah T, Mistar EM, Supardan MD. Porous structure and adsorptive properties of activated carbon derived from Bambusa vulgaris striata by two-stage KOH/NaOH mixture activation for Hg^{2+} removal. J Water Process Eng. 2021;43:102294. https://doi.org/10.1016/j.jwpe.2021.102294
50. Ding J, Meng Y, Lu S, Peng Y, Yan W, Li W, et al. The treatment of aquaculture wastewater with biological aerated filters: From the treatment process to the microbial mechanism. Toxics. 2023;11(6):478. https://doi.org/10.3390/toxics11060478
51. Zhang L, Zhai T, Yang M, Hu C. Few-layered $Bi_4O_5I_2$ nanosheets enclosed by {10−1} facets with oxygen vacancies for highly-efficient removal of water contaminants. J Hazard Mater. 2022;437:129274. https://doi.org/10.1016/j.jhazmat.2022.129274
52. Huang W, Tan Y, Zhang C, Zhou Q, Yang K, Zhang Y, et al. In situ decoration of $La(OH)_3$ on polyethyleneimine-linked dendritic mesoporous silica nanospheres targeting efficient and simultaneous removal of phosphate and Congo red. Environ Sci Nano. 2021;8:3792–805. https://doi.org/10.1039/D1EN00853F

CC BY

53. Lohwacharin J, Maliwan T, Osawa H, Takizawa S. Effects of ferrihydrite-impregnated powdered activated carbon on phosphate removal and biofouling of ultrafiltration membrane. Water. 2021;13(9):1178. https://doi.org/10.3390/W13091178
54. Pica M. Treatment of wastewaters with zirconium phosphate-based materials: A review on efficient systems for the removal of heavy metal and dye water pollutants. Molecules. 2021;26(8):2392. https://doi.org/10.3390/MOLECULES26082392
55. Nobaharan K, Bagheri S, Asgari N, Lajayer B, Van Hullebusch ED. Phosphorus removal from wastewater: The potential use of biochar and the key controlling factors. Water. 2021;13(4):517. https://doi.org/10.3390/W13040517
56. Nguyen MD, Adhikari S, Amini N, Mallya D, Thomas MW, Moon EM, Milne N. Phosphorus adsorption and organic release from dried and thermally treated water treatment sludge. Environ Res. 2023;234:116524. https://doi.org/10.1016/j.envres.2023.116524
57. Chu Z, Wang W, Yin M, Yang Z. Zirconium component modified porous nanowood for efficient removal of phosphate from aqueous solutions. Nanomaterials (Basel). 2023;13(11):1807. https://doi.org/10.3390/nano13111807
58. Vu M, Duong HC, Wang Q, Cai Z, Hoang BN, Viet NT, Nghiem LD. A low-cost method using steel-making slag to quench the residual phosphorus from wastewater effluent. Environ Technol Innov. 2023;31(8):103181. https://doi.org/10.1016/j.eti.2023.103181